Sensors and Materials, Vol. 35, No. 2 (2023) 411–422
MYU Tokyo

S & M 3177

Trajectory Planning Strategies and Simulation for Autonomous-surface-vehicle–Remotely-operated-vehicle (ASV–ROV) Cooperative System

Akihiro Morinaga* and Ikuo Yamamoto

Nagasaki University, 1-14 Bunkyo, Nagasaki City 852-8521, Japan

(Received January 6, 2023; accepted February 6, 2023)

Keywords: underwater robot, ROV, ASV, path planning, feedback control

With the increase in the number of offshore power generation facilities and aquaculture ponds, demand for remotely operated vehicles (ROVs) to inspect underwater structures and conduct ecological surveys is increasing. Because ROVs are connected to a ground station on the water by a tether cable to enable the transmission of operating commands and images underwater, where radio communication is difficult, they can only operate within the range of the tether cable. To expand the operational range of ROVs, an autonomous surface vehicle (ASV)–ROV cooperative system, in which a tether cable is connected to an ASV and radio waves are used for remote operation from the autonomous vessel, is attracting attention. In a cooperative system, the tether cable must be managed on the ASV side, and the position and cable length of the ASV must be controlled to prevent the cable from pulling against or tangling with the ROV, which moves around underwater under the command of a human controller. We propose a method of controlling the position and cable length of the ASV using the information on the position of the ROV obtained from an underwater positioning device for an ASV–ROV cooperative system that we are also developing. In addition, we confirmed through simulations that the ASV and cable length follow target values even when the ROV moves along a complicated path.

1. Introduction

In recent years, demand for underwater robots has been increasing for the purpose of underwater infrastructure inspection and environmental surveys. With the increase in the number of wind farms and aquaculture ponds, remotely operate vehicles (ROVs) are being actively used instead of divers to perform underwater monitoring.(1,2) Because radio communication is difficult underwater, the underwater vehicle is connected to a base station above the water by a tether cable that transmits operational commands and underwater images. The cable also serves as a lifeline for the ROV, allowing the ROV to be retrieved by hand if it malfunctions.

*Corresponding author: e-mail: a-morinaga@nagasaki-u.ac.jp
https://doi.org/10.18494/SAM4302

ISSN 0914-4935 © MYU K.K.
https://myukk.org/

However, the use of tether cables also has disadvantages in ROV operation. If the cable length is smaller than the distance between the ROV and the base station, the ROV will be pulled by the cable, making it impossible for it to achieve the movement intended by the operator. In addition, as the ROV moves around in the water, the cable can become entangled in the ROV's fuselage, surrounding reefs, or hull, causing fatal problems that in some cases make the ROV unrecoverable. The effect of the cable on the ROV cannot be ignored and has been evaluated through simulations and experiments.[3,4] To prevent the cable from interfering with the ROV's motion due to these problems, the length and direction of the cable feed must be adjusted appropriately according to the ROV's position and attitude. For large ROVs, such as those used in deep water, the base station is located on a larger workboat, making it difficult to unroll the cable from the vessel or manually manage the cable, so a tether management system (TMS), in which a cable drum is thrown into the sea, is used. In the case of commercially available small ROVs, the tether cable is connected to a cable drum on board or on land, and a person manages the length and direction of the cable depending on the position and attitude of the ROV. Cable management requires experience. In addition, the range that an ROV can search is limited to the distance that the cable can reach from the base station, which means that the operator must go offshore or along the coast by getting on a boat or by other means.

In recent years, to expand the range of activities of ROVs, attention has been focused on a cooperative system between ROVs and autonomous surface vehicles (ASVs),[5–11] in which an autonomous vessel and an ROV are connected by a tether cable. The autonomous vessel relays between the ROV and the base station to enable underwater observations by ROVs in areas far from the base station.

We have developed an ASV–ROV for surveying marine debris on remote islands. With this system, litter washed ashore can be photographed by a camera on the ASV, and underwater and seabed litter can be photographed by the ROV, enabling efficient surveys in areas where it is difficult for people to enter by land. Various ASV–ROV coordination systems have also been proposed; a simple small vessel with thrusters attached to a floating body has been combined with an ROV to survey shallow water areas,[6] and in this system, the small vessel is pulled by the ROV's motion and follows it. Because the cable is attached to the ASV side via a spring, no particular control of the cable is required. Anglerfish, which is an ASV-controlling ROV, has been developed, and a method of determining the cable length from the estimated position of the ROV has been proposed for a coordinated system between the ROV and the ASV, but it does not indicate the appropriate position on the ASV side. To analyze the motion of the cooperative system, it is necessary to model the cables.[12–15] Hong *et al.*[13] modeled the behavior of a tether cable in the sea using the lumped-mass method and showed the effect of the tether cable on the ROV in a simulation. However, these cable models are simplified models, and it is difficult to accurately estimate the shape of the cable in real time using the models. A method of considering the cable as a catenary curve for control has been proposed, but the cable between the ASV and the ROV has a catenary shape only in special cases.

We propose herein a method of controlling the position of the ASV and the cable length using the position information for the ROV obtained from the underwater positioning system for the ASV–ROV coordination system that we are developing. Instead of estimating and controlling the shape of the cable drifting in the sea, the ideal positional relationship between the ASV and the ROV and the cable length were determined, and the ASV and cable length were controlled using these as target values. We confirm that the ASV and cable length follow the complicated movement of the ROV in simulations using a kinematic model.

2. Specification of the ASV and ROV Cooperative System

This section describes the system shown in Fig. 1, in which the ASV and ROV cooperate. The system consists of an ROV that searches underwater, an ASV that carries a base station for the ROV and can itself navigate independently or be piloted remotely, and a cable drum that uses a motor to feed and unwind the tether cable.

2.1 ASV

The ASV in this system has two main thrusters for moving and four rhombus-shaped thrusters for fine fixed-point holding, and is capable of omni-directional turning movements. The body is 1400 mm × 1100 mm × 650 mm in size, and its weight is approximately 30 kg, which allows for operation by two people. It is also equipped with a global navigation satellite system (GNSS), enabling it to maintain a fixed point at sea and to navigate automatically by specifying coordinates. The ASV can be remotely operated from land, and the images from the cameras mounted on the ASV can be transmitted to an operator on land in real time via wireless communication. In addition, a basket for storing the ROV is installed between the left and right floats of the ASV, and the height of the basket can be adjusted so that the ROV does not act as a drag when the ASV is sailing.

2.2 ROV

The ROV connected to the ASV is small, measuring 470 mm × 450 mm × 200 mm and weighing less than 10 kg. The ROV is equipped with Pixhawk and RaspberryPi as controllers, and an XInput controller is generally used to control the ROV through QGroundControl.

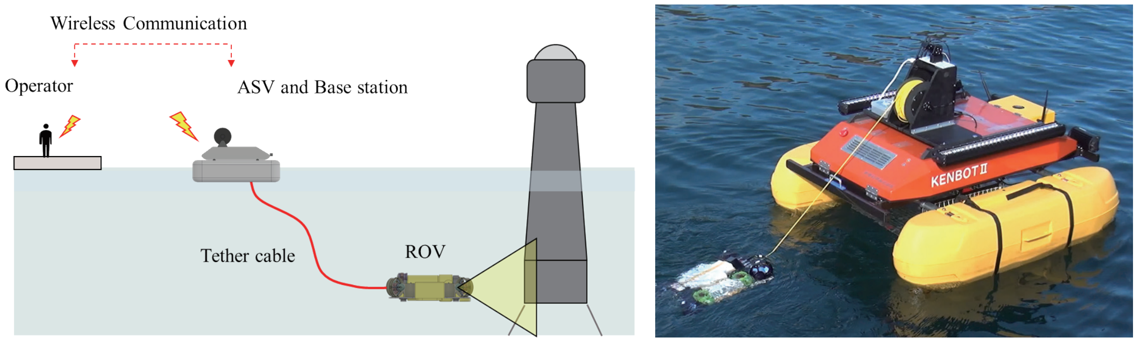

(a) (b)

Fig. 1. (Color online) (a) Concept of an ASV–ROV cooperative system and (b) actual vehicles.

However, this system must be operated remotely via wireless communication, and the XInput controller cannot be connected directly to the PC on the ASV. For this reason, Futaba's R3008SB is connected to the microcontroller (Arduino Pro Micro) to enable wireless communication and to receive radio signals from the land side as pulse width modulation (PWM) signals, and the microcontroller is used as the XInput controller to convert the radio signals so they may be recognized by QGroundControl. The QGroundControl is connected to the microcontroller.

2.3 Cable drum

The tether cable extending from the ROV is connected to the cable drum mounted on the ASV as shown in Fig. 2. From this cable drum, the cable is converted to an Ethernet cable through a slip ring and connected to the base station. The cable drum is rotated by a DC motor to automate the feeding and unwinding of the cable, which is usually performed by a person. When the drum is rotated passively, the electromagnetic clutch is turned OFF. A rotary encoder is attached to the rotation shaft of the cable drum, and the length of the deployed cable can be calculated from the rotation angle of the drum.

2.4 System configuration

To link ROVs and ASVs, relative location information is needed. Therefore, this system incorporates Shallow Compass 50, which is an acoustic positioning device. This device fixes a transponder that transmits sound waves to the ROV and the antenna that receives sound waves on the ASV, and by combining them with the depth information from the ROV, the relative position can be obtained.

(a) (b)

Fig. 2. (Color online) (a) ASV and ROV in the cooperative system, and (b) the cable drum.

The system configuration, including the ROV, ASV, and acoustic positioning device, is shown diagrammatically in Fig. 3. In this system, the ROV is operated by the operator, and the ASV moves autonomously according to the position and heading of the ROV. The ASV determines its movement from the relative position and azimuth of the ROV, as well as the cable length. The relative position of the ROV to the ASV is determined by an acoustic positioning system, which has a sampling rate of approximately 1 Hz.

3. Autonomous Control of ASV and Cable Length

3.1 Mathematical models

The coordinates shown in Fig. 4 are used to mathematically describe the positions of the ASV and ROV and the cable length. The term $\boldsymbol{\Sigma}_b$ is the reference coordinate, and $\boldsymbol{\Sigma}_a$ and $\boldsymbol{\Sigma}_r$ are coordinates fixed on the ASV and ROV, respectively. Both are assumed to be right-handed systems with the x-axis in the forward direction of the vehicle. For simplicity, the roll and pitch

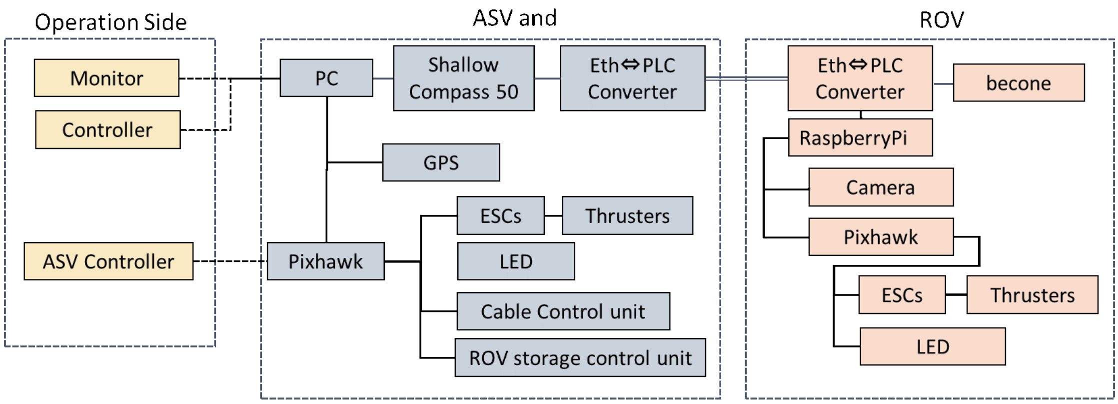

Fig. 3. (Color online) Configuration of cooperative system.

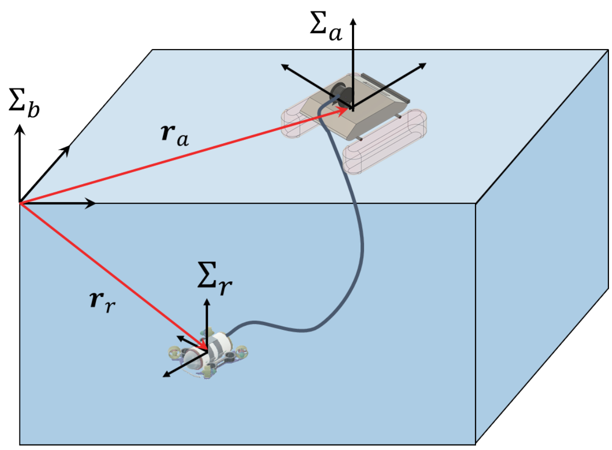

Fig. 4. (Color online) Coordinates and position vectors.

of the ASV and ROV are always assumed to be zero, and the vertical motion of the ASV is ignored. The position vector of the ASV is $\boldsymbol{r}_a = [x_a, y_a, 0]$; the position vector of the ROV, $\boldsymbol{r}_r = [x_r, y_r, z_r]$; and the orientations of the ASV and ROV are θ_a and θ_r, respectively. The term l is the cable length, not considering the part of the cable that is wrapped around the drum; therefore, $l \geq |\boldsymbol{r}_a - \boldsymbol{r}_r|$ and is zero when $\boldsymbol{r}_a = \boldsymbol{r}_r$.

The ASV can obtain thrust in three degrees of freedom (forward, backward, left, right, and turn) using six thrusters. Therefore, after setting the velocity of the three degrees of freedom as $[u_x, u_y, u_\theta]$, the kinematics of the ASV can be expressed as

$$\begin{bmatrix} \dot{x}_a \\ \dot{y}_a \\ \dot{\theta}_a \end{bmatrix} = \begin{bmatrix} \cos\theta_a & -\sin\theta_a & 0 \\ \sin\theta_a & \cos\theta_a & 0 \\ 0 & 0 & 1 \end{bmatrix} \begin{bmatrix} u_a \\ v_a \\ \omega_a \end{bmatrix}. \tag{1}$$

The ROV is equipped with eight thrusters and is assumed to be capable of arbitrary velocities for four DOF directions. Let the velocity of the ROV be $[v_x, v_y, v_z, v_\theta]$, then the kinematics of the ROV can be expressed as

$$\begin{bmatrix} \dot{x}_r \\ \dot{y}_r \\ \dot{z}_r \\ \dot{\theta}_r \end{bmatrix} = \begin{bmatrix} \cos\theta_r & -\sin\theta_r & 0 & 0 \\ \sin\theta_r & \cos\theta_r & 0 & 0 \\ 0 & 0 & 1 & 0 \\ 0 & 0 & 0 & 1 \end{bmatrix} \begin{bmatrix} v_x \\ v_y \\ v_z \\ v_\theta \end{bmatrix}. \tag{2}$$

If the drum rotation speed multiplied by the radius is u_l, the variation of the cable length over time is $\dot{l} = u_l$. Each of the velocities is constrained by the limitations of the thrust and the drum rotation speed. That is, $|u_x| \leq u_{x,max}$, and the same is true for the other seven velocities.

3.2 Strategy of control ASV and cable length

While the ROV is exploring in the sea, the ASV is required to adjust its position and orientation, the viewpoint from which the cable is unrolled, and the cable length to prevent the tether cable from tangling with the ROV or pulling the ROV and interfering with its motion. In addition, the cable length must be adjusted by controlling the cable drum. However, it is difficult to calculate under what conditions the cable may become entangled in the ROV and under what conditions tension may be generated against the ROV because a complete estimation of the shape of a cable deployed in the sea requires calculating the deformation of a flexible body under the influence of tidal currents, which is itself a very large problem. Furthermore, it is impractical to compute the shape of the cable, because it must be computed in real time for use in the control of the ASV.

We took advantage of the ability to freely move the cable steering position using the ASV as a base station and the plan for the ASV trajectory and control with the following policy.

First, as shown in Fig. 4, we assumed that if the ASV is always positioned directly behind and oriented with respect to the ROV, the cables will not become entangled. In other words, for the position of the ROV, $\boldsymbol{r}_r = [x_r, y_r, \theta_r]$, the target position of the ASV, $\boldsymbol{r}_r = [x_t, y_t, \theta_t]$, is determined as

$$\begin{cases} x_t = x_r - d\cos\theta_r \\ y_t = y_r - d\sin\theta_r \\ \theta_t = \theta_r \end{cases}, \tag{3}$$

where d is the horizontal distance between the ROV and the ASV and is determined by the depth of the ROV, $d = az_r$, $a > 0$.

Next, the target cable length l_t is determined by multiplying the distance between the ROV and the ASV by a constant plus a value proportional to the error in orientation between the ROV and the ASV.

$$l_t = \left\{\beta + \gamma\left(\theta_r^k - \theta_a\right)\right\}\left|\boldsymbol{r}_r - \boldsymbol{r}_a\right|, \tag{4}$$

where $\beta > 0$ and $\gamma > 0$ are coefficients for lengthening the cable according to the differences in linear distance and orientation. If the ASV and cable length always follow the target values in Eqs. (3) and (4), the cable is expected to approximate a catenary shape with the endpoints at the ASV and ROV as shown in Fig. 5. If the parameters β and γ in Eq. (4) are large, the cable becomes longer, and the shape changes owing to currents and the movement of the vehicles, increasing the likelihood of entanglement. On the other hand, if β and γ are small, $l < |\boldsymbol{r}_r - \boldsymbol{r}_a|$, which may adversely affect the motion of the ROV. Therefore, it is desirable to assume as small a value as possible, adjusting it according to the motion of the ROV and the environmental conditions.

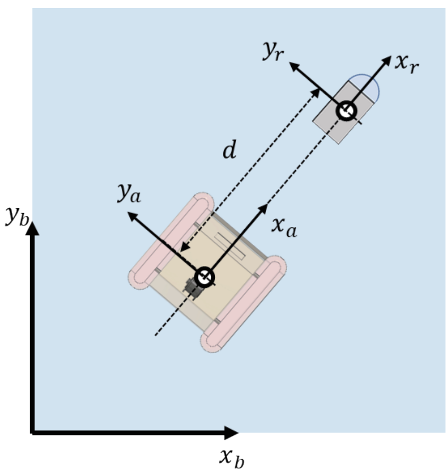

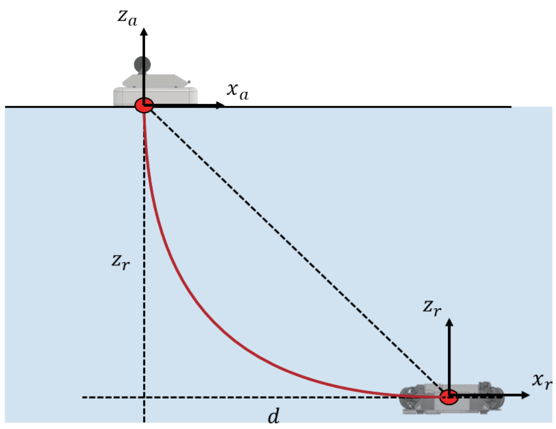

Fig. 5. (Color online) (a) Waypoint of ASV set behind the ROV and (b) setting the cable length.

3.3 Motion planning and control

Herein, we describe a method of controlling the ASV and cable length on the basis of the observed state variables with respect to the target values in Eqs. (3) and (4). The simplest method is to introduce feedback control using the values in Eqs. (3) and (4) as target values. If the values of each variable can be obtained by sensors at a high sampling rate and a large feedback gain can be taken, it is always possible to follow the target values. However, the maximum sampling rate of the underwater positioning device used to obtain the ROV's position is about 1 Hz. In addition, the speed of the ASV and the rotational speed of the cable drum have limitations, so the target value cannot be tracked if the ROV suddenly changes its orientation.

Therefore, the target position of the ASV, which is calculated from the position of the ROV obtained at regular intervals, is set as a waypoint, and trajectory tracking control is introduced in which trajectories with straight lines connect the waypoints obtained at each time. The position of the ROV obtained at time t_k is $\boldsymbol{r}_r^k$, and the waypoints $\boldsymbol{r}_w^k$ set at this time may be expressed as

$$\boldsymbol{r}_w^k = \begin{bmatrix} x_r^k - d\cos\theta_r^k \\ y_r^k - d\sin\theta_r^k \\ \theta_r^k \end{bmatrix}. \tag{5}$$

As time passes, waypoints are generated in sequence $\boldsymbol{r}_w^0$, ..., $\boldsymbol{r}_w^k$ from $t^0 = 0$ to $t^k = kT$. The ASV is always feedback-controlled with the waypoint with the smallest upper index as the target value. When the error between the current target value and the ASV becomes smaller than the allowable error, that is, when $\left|\boldsymbol{r}_w^k - \boldsymbol{r}_a(t)\right| < e$ is satisfied, the next numbered waypoint is changed to the new target. The behavior of ASVs and waypoints in this sequence is shown in Fig. 6. To control the cable length, the target cable length is calculated from Eq. (4) for the position data of the ROV $\boldsymbol{r}_r^k$ with the largest index k, and feedback control is applied.

4. Simulation

The behavior of the ASV and the cable length when the ASV and cable length control method proposed in Sect. 3 is applied was verified in a simulation versus the kinematic model in Eqs. (1) and (2). In an actual operation, the ROV moves on the basis of the speed command given by the operator. The actual speed is different from the commanded value because the ROV is affected by tidal currents and tether cable tension. For simplicity, we assume that the speed of the ROV can achieve a given speed command value by a sufficiently large thruster thrust, unaffected by currents or cable tension, and that its motion follows the kinematic equation [Eq. (2)]. The target values for the ASV and cable length were determined by assuming that the position of the ROV had a true value every second. A proportional (P)-controller was applied with respect to the target values. In addition, the upper limit of the speed of the ASV was $u_{x,max} = u_{y,max} = 3$ m/s, $u_{\theta,max} = 3$ rad/s, and the tolerance for determining that the ASV had reached the waypoint was set at $e = 0.01$.

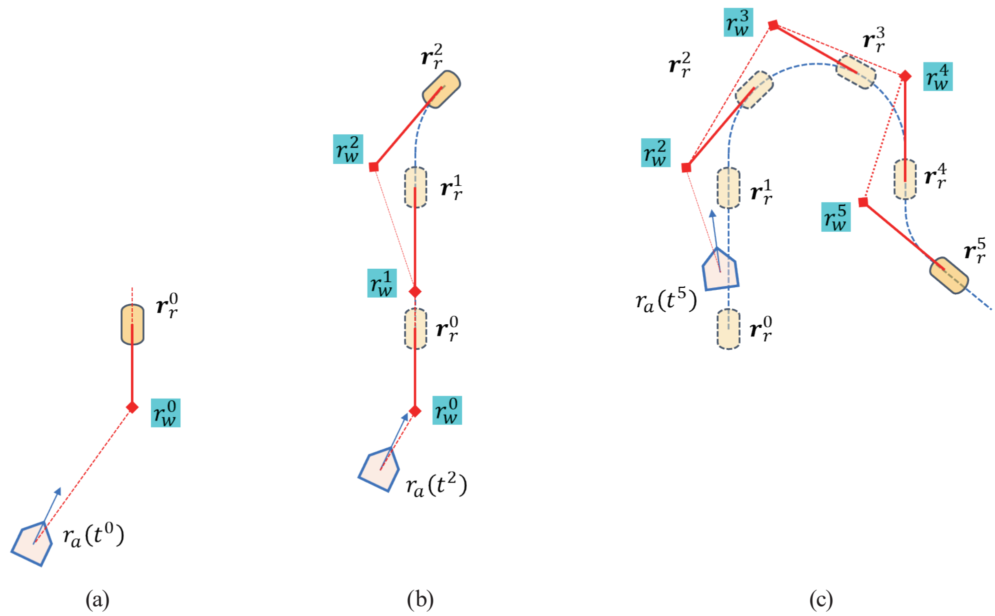

Fig. 6. (Color online) ASV control flow: (a) waypoints are set every time ROV positioning data is obtained, (b) waypoints are set one after another, but the oldest waypoint is the target, and (c) when the target waypoint is passed, the next waypoint is reset as the target of the ASV.

In this simulation, the velocity input of the ROV was set as shown in Fig. 7, with a constant translational velocity input every 5 s and a feedback input given at the target angle. The resulting motion of the ROV is shown by the red line in Fig. 8. The trajectory and time variations of the ASV and cable length when the control method described in previous section was applied are shown in Figs. 8–11. The solid blue line in Fig. 8 shows the trajectory of the ASV, and the circle marks the waypoints determined by the position of the ROV every second. The arrow indicates the forward direction of the ASV. When the error between the ASV and the target waypoint $\boldsymbol{r}_w^k$ is less than tolerance, the target waypoint was switched to $\boldsymbol{r}_w^{k+1}$. The dashed lines in Figs. 9 and 10 respectively indicate the target position and orientation at each time. The P-controller was applied to the cable length using the value in Eq. (3) as the target value, and the cable length always changed to a larger value relative to the linear distance between the ROV and the ASV shown by the red line in Fig. 11. Thus, when the proposed method was applied, the ASV always moved behind the ROV, even when the ROV performed complex motions, and the cable length could be varied to assume a value greater than the linear distance between the ROV and the ASV.

In this simulation, the controller of the ASV for the waypoints was a simple proportional control. This controller did not consider that the target value changed discontinuously as the waypoints were updated, nor did it consider input saturation. As a result, as seen in Fig. 8, the target value was moved away from the target value on the way from waypoint 7 to waypoint 8, and, as seen in Fig. 11, the change in cable length oscillated. Considering the operation of motors that rotate thrusters and cable drums in actual ASVs, the control controller must be improved. Furthermore, the shape and tension of the cable were not considered in this simulation, so it is

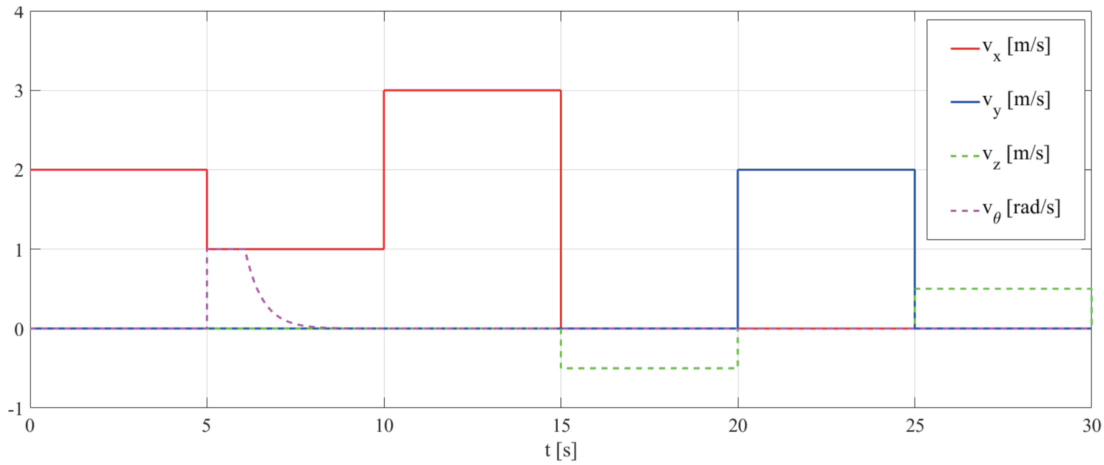

Fig. 7. (Color online) Velocity of ROV over time.

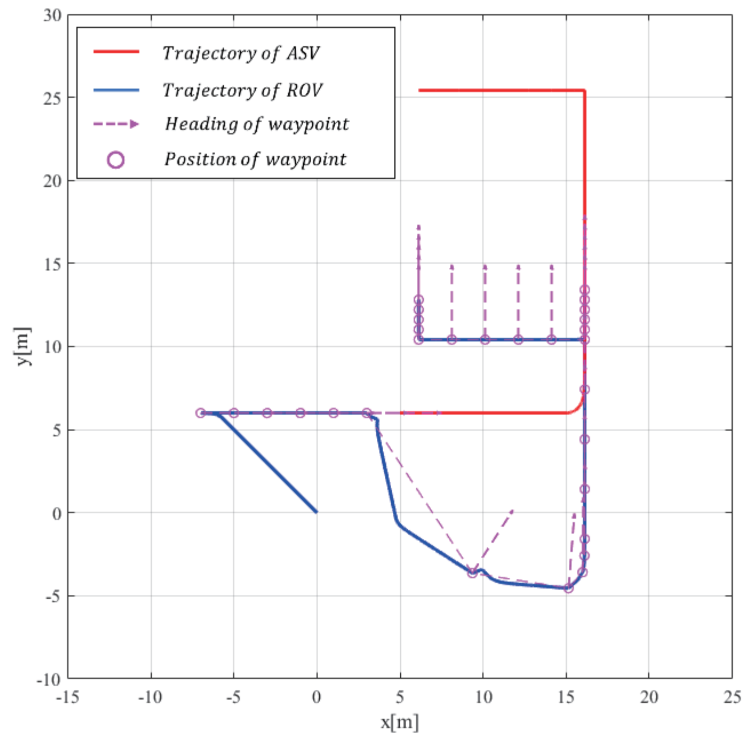

Fig. 8. (Color online) Trajectories of ASV and ROV on an x–y plane. Small circles and arrows on the blue trajectory line denote the position and heading of waypoints, respectively.

not possible to check whether the cable became tangled. It is conceivable that an equation of motion for the cable could be established and verified by simulation, but it is difficult to calculate the correct shape of the cable with existing models. Furthermore, because it is difficult to mathematically define whether cables became entangled, we plan to test the effectiveness of the proposed method, including cables, through experiments with actual machines. It is also necessary to verify the method of determining the parameters included in Eq. (4).

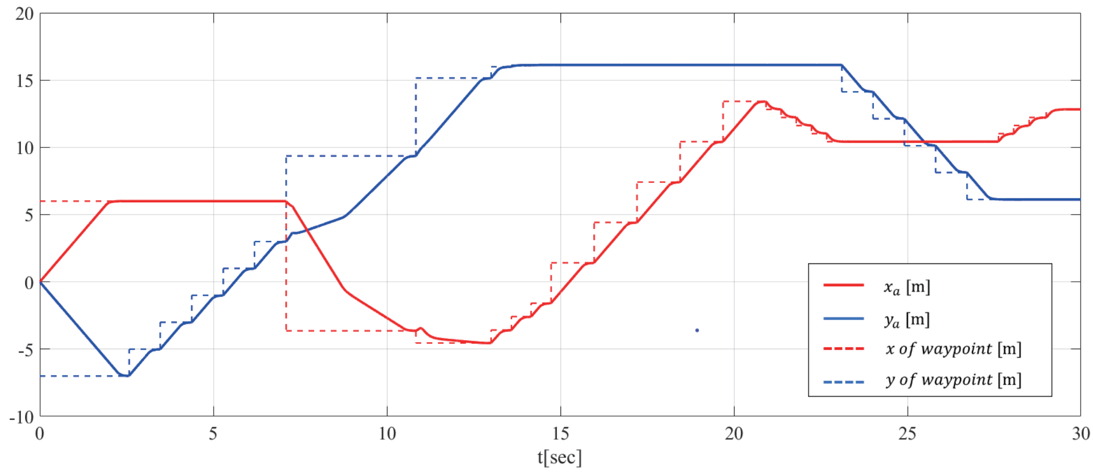

Fig. 9. (Color online) Position of ASV over time. Dashed lines denote the position of the target waypoint at each time, which corresponds to each circle in Fig. 8.

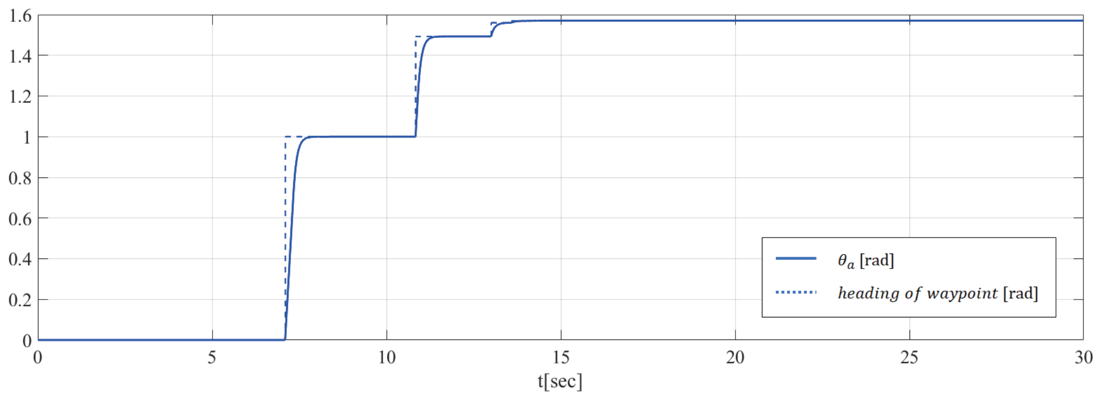

Fig. 10. (Color online) Orientation of ASV over time and orientation of waypoints at each time.

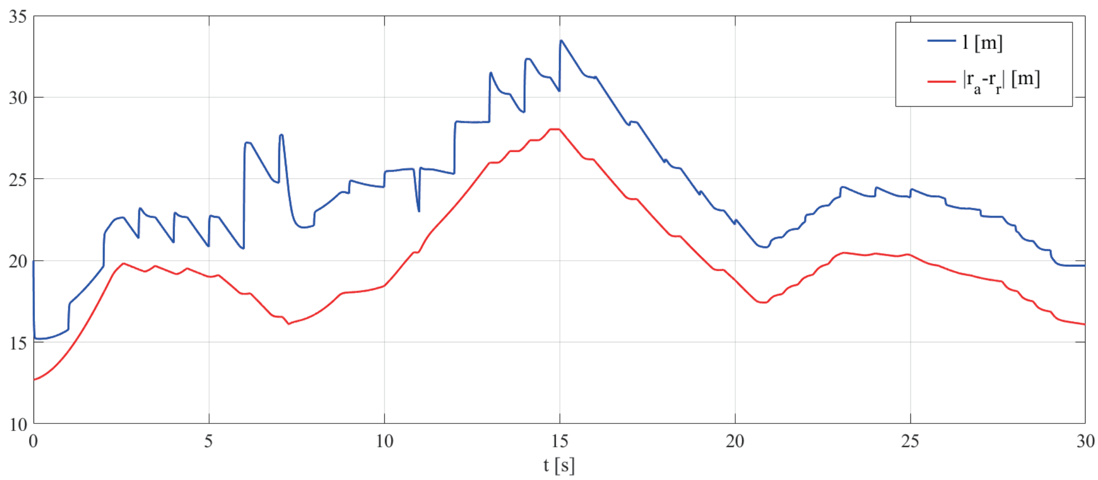

Fig. 11. (Color online) Cable length and distance between ASV and ROV over time.

5. Conclusions

We proposed a method of controlling the position of an ASV and the cable length using the position information from an ROV obtained from the underwater positioning system for an ASV–ROV coordination system. Instead of estimating and controlling the shape of the cable drifting in the sea, the ideal positional relationship between the ASV and ROV and the cable length were determined and the ASV and cable length can follow target values. In addition, the effectiveness of the proposed method was confirmed by simulations on a kinematic model. In the future, the proposed method will be implemented on actual vehicles and verified through experiments.

References

1 C. Masuzaki, I. Yamamoto, A. Morinaga, K. Sadano, Y. Kai, T. Nakano, and Y. Kato: Sens. Mater. **33** (2021) 907. https://doi.org/10.18494/SAM.2021.3223
2 R. Capocci, G. Dooly, E. Omerdić, J. Coleman, T. Newe, and D. Toal: J. Marine Sci. Eng. **5** (2017) 13. https://doi.org/10.3390/jmse5010013
3 Z. Feng and R. Allen: Ocean Eng. **31** (2004) 1019. https://doi.org/10.1016/j.oceaneng.2003.11.001
4 S. Yamaguchi, Y. Mizoguchi, and R Sakamoto: J. Jpn. Soc. Nav. Archit. Ocean Eng. **25** (2017) 143. https://doi.org/10.2534/jjasnaoe.25.143
5 A. Gray and E. Schwartz: Proc. 29th Florida Conf. Recent Advances in Robotics (FCRAR, 2016) 105.
6 G. Conte, D. Scaradozzi, and N. Ciuccoli: Adv. Rob. Mech. Eng. **2** (2020) 217. https://doi.org/10.32474/arme.2020.02.000150
7 M. Laranjeira, C. Dune, and V. Hugel: Ocean Eng. **200** (2020). https://doi.org/10.1016/j.oceaneng.2020.107018
8 C. Zhao, P. R. Thies, and L. Johanning: Ocean Eng. **259** (2022). https://doi.org/10.1016/j.oceaneng.2022.111899
9 C. Zhao, P. R. Thies, and L. Johanning: Appl. Ocean Res. **115** (2021) 102827. https://doi.org/10.1016/j.apor.2021.102827
10 C. Zhao, P. Thies, J. Lars, and J. Cowles: Ocean Eng. **232** (2021) 109019. https://doi.org/10.1016/j.oceaneng.2021.109019
11 G. Conte, D. Scaradozzi, D. Mannocchi, P. Raspa, L. Panebianco, and L. Screpanti: IFAC-PapersOnLine **49** (2016) 347. https://doi.org/10.1016/j.ifacol.2016.10.428
12 N. Lv, J. Liu, H. Xia, J. Ma, and X. Yang: Comput.-Aided Des. **122** (2020) 102826. https://doi.org/10.1016/j.cad.2020.102826
13 S. M. Hong, K. N. Ha, and J. Y. Kim: J. Mar. Sci. Eng. **8** (2020) 318. https://doi.org/10.3390/jmse8050318.
14 M.-C. Fang, C.-S. Hou, and J.-H. Luo: Ocean Eng. **34** (2007) 1275. https://doi.org/10.1016/j.oceaneng.2006.04.014.
15 T. Philipp, L. Dongwon, T. Felix, and P. Andreas: Cable-Driven Parallel Robots (Springer, Cham, 2019) pp. 295–306.